Open access • Journal Article • DOI:10.1109/TIP.2017.2700765

Joint Source-Channel Coding of JPEG 2000 Image Transmission Over Two-Way Multi-Relay Networks — Source link

Chongyuan Bi, Jie Liang

Institutions: Simon Fraser University

Published on: 03 May 2017 - IEEE Transactions on Image Processing (IEEE)

Topics: Lossless JPEG, JPEG 2000, Variable-length code, Transform coding and Shannon–Fano coding

Joint Source-Channel Coding of JPEG 2000 Image Transmission Over Two-Way Multi-Relay Networks

Chongyuan Bi, and Jie Liang

***Abstract*—In this paper, we develop a two-way multi-relay scheme for JPEG 2000 image transmission. We adopt a modified time-division broadcast (TDBC) cooperative protocol, and derive its power allocation and relay selection under a fairness constraint. The symbol error probability of the optimal system configuration is then derived. After that, a joint source-channel coding (JSCC) problem is formulated to find the optimal number of JPEG 2000 quality layers for the image and the number of channel coding packets for each JPEG 2000 codeblock that can minimize the reconstructed image distortion for the two users, subject to a rate constraint. Two fast algorithms based on dynamic programming (DP) and branch and bound (BB) are then developed. Simulation demonstrates that the proposed JSCC scheme achieves better performance and lower complexity than other similar transmission systems.**

***Index Terms*—Joint source-channel coding, two-way multi-relay system, relay selection, power allocation, JPEG 2000.**

I. Introduction

In this paper, we study wireless multimedia transmission between two users. Many applications fit into this scenario, such as video conference, live chatting, and live streaming. Since wireless channels are usually unreliable and have limited bandwidth due to fading, path loss and additive noise, how to transmit the multimedia between two users in real time with high reliability is a challenging problem [1]. This usually requires techniques from both source coding and channel coding, i.e., joint source-channel coding (JSCC), so that we can generate efficient and error resilient codestreams.

We focus on JPEG 2000-based image transmission [2]. JPEG 2000 is a powerful wavelet-based image coding standard, which can generate embedded codestreams. It also provides a number of error-resilient (ER) tools to improve the robustness of the codestream, which is very helpful to the applications studied in this paper. The framework developed in this paper can also be extended to video applications using Motion JPEG 2000 [3].

On the other hand, as wireless devices become ubiquitous and more powerful, user cooperation or wireless relaying has been proposed to provide spatial diversity and improve the performance of wireless communications [4], [5], where a device can serve as a relay to help the communications of other devices. Earlier works in this field focused on developing one-way cooperative protocols [5]. Since two-way communication is required in many applications, several efficient two-way relay protocols have also been developed [6].

In the rest of this paper, we first discuss related work and highlight our main contributions in Sec. II. In Sec. III, we develop a two-way multi-relay system to transmit JPEG-2000-coded images. The proposed system uses a modified time-division broadcast (TDBC) protocol, and operates in two-phase or three-phase mode, depending on the achievable sum data rate of the two users. We study the corresponding optimal power allocation and relay selection under a fairness constraint to maximize the sum rate of the system. In Sec. IV, we derive the symbol error probability (SEP) of the system under the optimal system configuration, from which we formulate in Sec. V a JSCC problem for the transmission of JPEG 2000 images. The goal is to optimally allocate source coding and channel coding rates to maximize the reconstructed image quality at the receiver under a total rate constraint. An exhaustive search (ES) method is firstly used to obtain the optimal solution as the ground truth. A dynamic programming (DP) method and a branch and bound (BB) algorithm are then developed to find near-optimal solutions with lower complexity. In Sec. VI, experimental results are reported to show the effectiveness of the proposed system and the JSCC approach. Finally, conclusions are drawn in Sec. VII.

II. Related Work and Our Contributions

A. Cooperative Protocols for Two-Way Relay Networks

Cooperative communication can combat channel fading, facilitate robust transmission, extend coverage and provide higher throughput in both wireless and mobile networks [5]. There are mainly two types of cooperative protocols for two-way relay networks, namely the two-phase multiple-access broadcast (MABC) and the three-phase time-division broadcast (TDBC) protocols [7].

In the two-phase MABC protocol, both users transmit their own signals to the relay in Phase 1, then the relay processes the received signals from the two users and broadcasts the combined signal back to them in Phase 2. In the three-phase TDBC protocol, User 1 first broadcasts its signal to the relay and User 2 in Phase 1. In phase 2, User 2 broadcasts its signal to the relay and User 1. Finally, the relay broadcasts the processed signal received from the first two phases back to the two users in Phase 3. In this paper, TDBC protocol with analog network coding (ANC) is used [8].

Both protocols have some drawbacks: MABC does not utilize the direct link between the two users. Therefore it has less degrees of freedom than TDBC. On the other hand, TDBC

This work was supported by the Natural Sciences and Engineering Research Council (NSERC) of Canada under grants RGPIN312262, STPGP380875, STPGP447223 and RGPAS478109. Corresponding author: J. Liang.

The authors are with the School of Engineering Science, Simon Fraser University, Burnaby, BC, Canada. Email: {cba30, jiel}@sfu.ca.

requires three phases to complete one frame's transmission, which decreases the spectral efficiency.

When there are multiple relays in two-way relay networks, there are many papers in the literature on relay selection, e.g., [9], [10], where only the best relay is used to forward messages. In this case, there is no interference issue and the complexity of the system can be simplified. However, these relay selection schemes are based on equal power allocation (EPA). In [11], the authors proposed a joint relay selection and power allocation scheme to maximize the minimum received SNRs of the two users under a total transmit power budget. In [12], another joint relay selection and power allocation scheme is proposed to minimize the symbol error probability (SEP). There are other schemes that minimize the outage probability or the total power, or maximize the sum rate [13], [14]. However, the aforementioned schemes do not consider data rate fairness between the two users. In real-time image/video communications, this may cause severe degradation of the quality of service (QoS) for one user. In [15], a power allocation method is developed for two-way relay networks that considers the data rate fairness constraint. However, only one relay is considered in it.

In this paper, we adopt a modified TDBC protocol. As discussed above, TDBC protocol decreases the spectral efficiency due to the three-phase transmission. To improve the spectral efficiency, when the direct link is good enough, we only use the first two phases of TDBC. Otherwise, the standard three-phase TDBC is used. We derive the optimal relay selection and power allocation for this modified framework. Note that since our goal is to design a two-way transmission framework for multimedia transmission, the two users have the same importance. Hence data fairness constraint is considered in the optimization.

B. Joint Source-Channel Coding for JPEG 2000

The joint source-channel coding (JSCC) for JPEG 2000 image transmission has been studied extensively [16]–[35]. In [16], a combined source and channel coding method is proposed to provide robust transmission of JPEG 2000 codestream over binary symmetric channels (BSC). Specifically, the source and channel codes are jointly optimized to produce a stream of fixed-size channel packets while maintaining full JP2 compliance. In [17], an adaptive unequal channel protection technique is proposed for JPEG 2000 codestream transmission over Rayleigh-fading channels, where the concatenation of a cyclic redundancy check code and a rate-compatible convolutional code is employed to design the unequal channel protection scheme. In [19], the priority encoding transmission framework is leveraged to exploit both unequal error protection and limited retransmission for rate-distortion-optimized delivery of streaming media. In [21], the transmission of scalable compressed data source over erasure channels is considered, and an unequal erasure protection algorithm is proposed. The proposed scheme is adapted to data with tree-structured dependencies. In [29], a unequal error protection (UEP) strategy is proposed for progressive JPEG 2000 codestream not only at the target transmission rate but also at the intermediate rates. A JSCC scheme is proposed in [30] for JPEG 2000 transmission over memoryless wireless channels, and the proposed JSCC scheme uses JPEG 2000 coding pass as the basic optimization unit. In [31], a product-code that consists of turbo code and Reed-Solomon code is employed for JPEG 2000 codestream protection over wireless channels, where the product-code is optimized by an iterative process. A dynamic channel coding scheme is presented for robust transmission of JPEG 2000 codestreams over mobile ad-hoc networks (MANET) in [32], and the proposed scheme is implemented according to the recommendations of the Wireless JPEG 2000 standard. In [33], a fast rate allocation method is presented for JPEG 2000 videos over time-varying channels, and the steepest descent algorithm is employed to extend the complexity scalability. Another UEP scheme is adopted for JPEG 2000 image/video transmission over wireless channel in [34]. The UEP method adopts a dichotomic technique for searching the optimal UEP strategy, and a virtual interleaving scheme is employed to reduce the effects of burst errors. In [35], a JSCC method for JPEG 2000 transmission over fading channels is proposed, and rate-compatible low-density parity-check (RCPC) code is employed with embedded codestream.

The aforementioned papers can be generally classified based on three criteria. The first one is the channel code they used, i.e., LDPC code, RCPC code, turbo code, and RS code. The second one is the channel they aim to transmit, i.e., BSC, memoryless channels, and fading channels. The third one is the JSCC solution they adopted, i.e., dynamic programming (DP), greedy method, Viterbi algorithm (VA), brute-force search, and bisection search.

In this paper, our objective is to transmit progressive and error-resilient JPEG 2000 codestreams over two-way multi-relay systems. A low-complexity JSCC approach is proposed, which exploits the error-resilient tools provided by JPEG 2000. We then develop a fast dynamic programming (DP) solution and a branch and bound (BB) solution to optimize the JSCC problem iteratively. Simulation results show that our method either has better performance than other methods, or has comparable performance but with lower complexity.

C. JPEG 2000 Transmission over Two-Way Relay Networks

The theoretical advantage of integrating cooperative communication and progressive image coding has been studied in [36]–[39]. Based on these analyses, several works have been proposed to study the image/video transmission over one-way cooperative communication channels [40]–[42]. Recently, there have been some works on two-way cooperative multimedia transmission [43], [44]. In [45], the authors proposed a video multicast system by integrating randomized distributed space-time coding (R-DSTC), packet-level FEC and network coding (NC). Further, in [43], they extend the work to a two-way relay video communication system. However, this system has some drawbacks. First, the packet-level FEC depends on simulated channel bit error rate (BER), which requires Monte Carlo simulations. Secondly, it applies FEC code uniformly over all packets, without considering the different error sensitivities of different parts of the video codestream. Moreover,

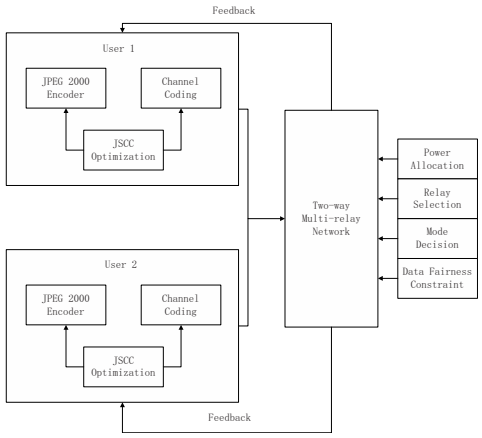

Fig. 1. Overview of the proposed system.

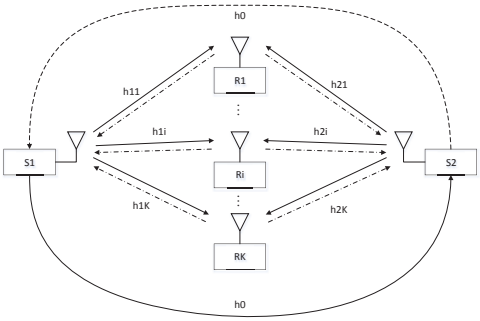

Fig. 2. Two-way multi-relay system.

the R-DSTC needs all relay nodes to cooperate, which has high complexity. In [44], the authors proposed an iterative joint source and channel coded modulation (JSCCM) scheme for robust video transmission over two-way relaying channels. The system consists of two users and one twin-antenna relay node. For each user the proposed video scheme includes a variable length code (VLC) encoder and two turbo trellis-coded modulation (TTCM) encoders, one at the source node and one at the relay node.

In this paper, we propose a two-way multi-relay system with joint mode selection, power allocation, and relay selection. We also consider a data rate fairness constraint. The system is then combined with our JSCC scheme for JPEG 2000 codestream transmission. The proposed two-way multi-relay transmission system can be adopted in any existing relay system or protocol without requiring any particular coding method, and the proposed JSCC scheme has low complexity and provides a better tradeoff between complexity and performance.

III. Two-way Multi-Relay System with Joint Optimization

A. System Model

The overall block diagram of our proposed system is shown in Fig. 1, where two users exchange information with the help of multiple relays. Each user has a JSCC optimization module, which optimizes the JPEG 2000 source encoder and channel coding. The optimized codestreams of the two users are transmitted over the two-way multi-relay network, which operates by jointly considering the power allocation, relay selection and mode decision under a fairness constraint.

The details of the two-way multi-relay module is shown in Fig. 2, where the two users are denoted by S_1 and S_2, and the K half-duplex relay nodes are denoted by $R_i, i = 1, 2, \cdots, K$. All relays use the amplify-and-forward (AF) protocol [46]. All channels are assumed to be quasi-static Rayleigh fading channels, i.e., the channels remain constant within one frame of transmission and change independently from one frame of transmission to another. We also assume all channels are reciprocal. The channel coefficients of links S_1S_2, S_1R_i, R_iS_2 are denoted by $h_0 \sim \mathcal{CN}(0, \theta_0)$, $h_{1i} \sim \mathcal{CN}(0, \theta_{1i})$, and $h_{2i} \sim \mathcal{CN}(0, \theta_{2i})$ respectively. We assume that both users and all relays are aware of all the channel state information (CSI) $\{h_0, h_{1i}, h_{2i}, i = 1, \cdots, K\}$, as in most papers on two-way relay networks [47]. The additive noise at receiving node l is denoted as $n_l \sim \mathcal{CN}(0, N_0)$, $l = S_1, S_2, R_i$. The transmission power of users S_1, S_2 and the i-th relay node are denoted as P_1, P_2 and P_{R_i}, respectively. The total power of the system is $P_1 + P_2 + P_{R_i} \leq P_T$, where P_T is the maximal total power of the system. The maximum ratio combining (MRC) method is employed at a user to combine the received signals from the other user and the relay [48]. BPSK modulation is considered throughout this paper, although the proposed system can be easily extended to other modulation schemes.

The TDBC protocol can efficiently utilize the direct link between the two users, but requires three phases of transmission per frame, which has lower spectral efficiency. Inspired by the incremental cooperation [46], in this paper, we design a modified TDBC protocol, which adaptively selects between the two-phase and the three-phase modes. The differences between our proposed modified TDBC protocol and the incremental cooperation are as follows. First, the incremental cooperation in [46] is designed for one-way relay protocol, whereas our proposed modified TDBC protocol is designed for two-way relay transmission. Second, the incremental cooperation uses the SNR of the source-destination link to decide whether the relay will be used or not. In our method, the sum rate is used as the metric to choose two-phase or three-phase mode. Third, our proposed method includes power allocation and the relay selection under a data rate fairness constraint, which is designed for multi-relay scenario, but the incremental cooperation in [46] only considers single relay case.

We first compute the achievable sum data rates for the two cases after power allocation and relay selection, by considering a data rate fairness constraint. If the achievable sum rate of the three-phase mode is higher than the two-phase mode, the conventional TDBC protocol is chosen, *i.e.*, a relay will be selected, which will broadcast the combined signal from the first two phases back to the two users in Phase 3. Otherwise, no relay will be used, and a new frame will start. Hence one phase is saved compared to TDBC protocol to improve the spectral efficiency. Note that, the decision of mode selection is made before the transmission of the first phase. Further, as all nodes have the knowledge of all CSIs, each user can compute the power of its own individually. In other words, the joint optimization can be employed in a distributed manner.

B. Sum Rate of the Two-Phase Mode

We first present the signals received by each node of the system after the first two phases. In Phase 1, S_1 broadcasts signal x_1 to S_2 and all relay nodes. The received signals at S_2 and R_i are

$$\begin{aligned} y_{S_1S_2} &= \sqrt{P_1}h_0x_1 + n_{S_2}, \\ y_{S_1R_i} &= \sqrt{P_1}h_{1i}x_1 + n_{R_i}. \end{aligned} \tag{1}$$

In Phase 2, S_2 broadcasts signal x_2 to S_1 and all relay nodes, S_1 and R_i receive

$$\begin{aligned} y_{S_2S_1} &= \sqrt{P_2}h_0x_2 + n_{S_1}, \\ y_{S_2R_i} &= \sqrt{P_2}h_{2i}x_2 + n_{R_i}. \end{aligned} \tag{2}$$

If we use two-phase mode, the sum data rate of the system is given by

$$R_{sum}^{(2)} = \frac{1}{2}\log_2(1+SNR_{21}^{(2)}) + \frac{1}{2}\log_2(1+SNR_{12}^{(2)}), \tag{3}$$

where he pre-log factor $\frac{1}{2}$ is due to the two-phase transmission, $SNR_{21}^{(2)}$ and $SNR_{12}^{(2)}$ are the received SNRs at users S_1 and S_2. Note that, the $SNR^{(i)}$ denotes SNR of phase i. From Eq. (1) and Eq. (2), we have

$$\begin{aligned} SNR_{21}^{(2)} &= \frac{|h_0|^2P_2}{N_0}, \\ SNR_{12}^{(2)} &= \frac{|h_0|^2P_1}{N_0}. \end{aligned} \tag{4}$$

In this paper, we want to ensure the data rate fairness between the two users. Since no relay is used in two-phase mode, it can be seen from Eq. (3) that the power should be equally allocated between the two users in order for them to have the same data rate, *i.e.*, $P_1 = P_2$ in two-phase mode.

In the proposed system, the sum rate of the two-phase mode will be compared to that of the three-phase mode to find the optimal mode. The three-phase mode will be described next.

C. Sum Rate of the Three-Phase Mode

For the three-phase mode, to find the optimal sum rate, we need to perform power allocation and relay selection. Suppose R_i is the selected relay, which combines the received signals from the first two phases as

$$\begin{aligned} y_{R_i} &= y_{S_1R_i} + y_{S_2R_i} \\ &= \sqrt{P_1}h_{1i}x_1 + \sqrt{P_2}h_{2i}x_2 + 2n_{R_i}. \end{aligned} \tag{5}$$

The combined signal is then multiplied by a normalization factor w_i to satisfy the power constraint of relay R_i, where w_i is given by

$$w_i = \sqrt{\frac{P_{R_i}}{P_1|h_{1i}|^2 + P_2|h_{2i}|^2 + 2N_0}}. \tag{6}$$

The scaled signal is then broadcasted back to the two users. The signals received at users S_1 and S_2 are given by

$$\begin{aligned} y_{S_1} &= h_{1i}w_iy_{R_i} + n_{S_1}, \\ y_{S_2} &= h_{2i}w_iy_{R_i} + n_{S_2}. \end{aligned} \tag{7}$$

After self-interference cancellation, the residual signals $\hat{y}_{S_1}$ and $\hat{y}_{S_2}$ can be found to be

$$\begin{aligned} \hat{y}_{S_1} &= \sqrt{P_2}h_{1i}h_{2i}w_ix_2 + 2h_{1i}w_in_{R_i} + n_{S_1}, \\ \hat{y}_{S_2} &= \sqrt{P_1}h_{2i}h_{1i}w_ix_1 + 2h_{2i}w_in_{R_i} + n_{S_2}. \end{aligned} \tag{8}$$

As MRC is used to combine the signals from the direct link and the selected relay node, the total received SNRs at S_1 and S_2 are

$$\begin{aligned} SNR_{21}^{(3)} &= SNR_{21}^{(2)} + \frac{P_2|h_{1i}|^2|h_{2i}|^2w_i^2}{4|h_{1i}|^2w_i^2N_0 + N_0}, \\ SNR_{12}^{(3)} &= SNR_{12}^{(2)} + \frac{P_1|h_{2i}|^2|h_{1i}|^2w_i^2}{4|h_{2i}|^2w_i^2N_0 + N_0}. \end{aligned} \tag{9}$$

The corresponding sum data rate is thus

$$R_{sum}^{(3)} = \frac{1}{3}\log_2(1+SNR_{21}^{(3)}) + \frac{1}{3}\log_2(1+SNR_{12}^{(3)}), \tag{10}$$

where the pre-log factor $\frac{1}{3}$ is due to the three-phase transmission.

In this paper, different from other papers, our goal is to maximize the sum rate with a data rate fairness constraint. Therefore we need to solve the following joint power allocation and relay selection problem.

$$\begin{aligned} \max_{R_i\in\mathcal{R},P_i} \quad & R_{sum}^{(3)} \\ s.t. \quad & SNR_{21}^{(3)} = SNR_{12}^{(3)}, \\ & P_1 + P_2 + P_{R_i} \le P_T, \\ & P_i \ge 0. \end{aligned} \tag{11}$$

where P_1, P_2, P_{R_i} are the allocated powers for the two users and the selected relay, and $\mathcal{R}$ is the relay candidate set.

Since only the selected relay transmits at Phase 3, we only need to focus on the power allocation problem with respect to the selected relay. Therefore, the power allocation problem can always be solved independently from the relay selection problem. As long as we have the solutions to the separate power allocation problem, we can then use the CSIs of the candidate relays to compute the relevant achievable sum data rate, and the relay selection problem can be solved accordingly. In this way, the joint optimization can be decoupled into two individual optimization problems, i.e., power allocation and relay selection. In the following, we solve the two optimization problems separately.

Since logarithm does not change the optimization result, the power allocation problem can be written as

$$\begin{aligned} \max_{P_i} \quad & \min(SNR_{21}^{(3)}, SNR_{12}^{(3)}) \\ s.t. \quad & P_1 + P_2 + P_{R_i} \le P_T, \\ & P_i \ge 0. \end{aligned} \tag{12}$$

Note that, $SNR_{21}^{(3)} = SNR_{12}^{(3)}$ is required at the optimum.

Let $f_0 = |h_0|^2$, $f_1 = |h_{1i}|^2$ and $f_2 = |h_{2i}|^2$. We next solve (12) by two methods, a solution using Karush-Kuhn-Tucker (KKT) conditions and an approximation method.

1) KKT Solution of Eq. (12): In this section, we present a KKT solution for Eq. (12). By introducing an intermediate variable v, the max-min problem Eq. (12) can be converted into a max problem, which is

$$\begin{aligned} \max_{P_i} \quad & v \\ s.t. \quad & SNR_{21} \geq v, \\ & SNR_{12} \geq v, \\ & P_1 + P_2 + P_{R_i} \leq P_T, \\ & P_i \geq 0. \end{aligned} \tag{13}$$

Since the objective function and constraints are all differentiable, the KKT necessary conditions [49] can be used to determine the optimal power allocation. To simplify the usage of the KKT conditions, we first transform Eq. (13) into an equivalent minimization problem as follows

$$\begin{aligned} \min_{P_i} \quad & -v \\ s.t. \quad & SNR_{12} - v \geq 0, \\ & SNR_{21} - v \geq 0, \\ & P_1 + P_2 + P_{R_i} - P_T \leq 0, \\ & P_i \geq 0. \end{aligned} \tag{14}$$

For ease of presentation, let $P_{R_i} = P_3$, the Lagrangian function of Eq. (14) is given by

$$\begin{aligned} &\mathcal{L}(P_1, P_2, P_{R_i}, v, \lambda_1, \lambda_2, \lambda_3, \lambda_4, \lambda_5, \lambda_6) = \\ &\quad -v - \sum_{k=1}^{3} \lambda_k P_k - \lambda_4 (SNR_{12} - v) \\ &\quad -\lambda_5 (SNR_{21} - v) + \lambda_6 (\sum_{k=1}^{3} P_k - P_T), \end{aligned} \tag{15}$$

where λ_k, $k = 1, 2, \cdots, 6$, are Lagrangian multipliers. The corresponding KKT conditions are then given by

$$-\lambda_k - \lambda_4 \frac{\partial SNR_{12}}{\partial P_k} - \lambda_5 \frac{\partial SNR_{21}}{\partial P_k} + \lambda_6 = 0, \quad k = 1, 2, 3, \tag{16}$$

$$-1 + \lambda_4 + \lambda_5 = 0 \tag{17}$$

$$\lambda_k \geq 0, \quad k = 1, 2, \cdots, 6 \tag{18}$$

$$\lambda_k P_k = 0, \quad P_k \geq 0, \quad k = 1, 2, 3 \tag{19}$$

$$\lambda_6 (\sum_{k=1}^{3} P_k - P_T) = 0, \quad \sum_{k=1}^{3} P_k \leq P_T, \tag{20}$$

$$\lambda_4 (SNR_{12} - v) = 0, \quad SNR_{12} \geq v, \tag{21}$$

$$\lambda_5 (SNR_{21} - v) = 0, \quad SNR_{21} \geq v. \tag{22}$$

Since our objective is to maximize the sum rate for the two users under fairness constraint, none of the three powers should be zero. From Eq. (13), all powers are positive. We then have $\lambda_1 = \lambda_2 = \lambda_3 = 0$. From Eq. (21) and (22), we have $SNR_{12} = SNR_{21}$. Hence, there are six equations for six variables $\lambda_4, \lambda_5, \lambda_6, P_1, P_2, P_3$.

Without loss of generality, we set $N_0 = 1$. By eliminating the extra variables, Eq. (16) to (22) can be written as

$$\begin{aligned} &\lambda_4 f_1 f_2^2 P_1 P_3 A^2 - \lambda_5 (f_0 A^2 B^2 + f_1 f_2 P_3 A B^2 \\ &- f_1 f_2^2 P_2 P_3 B^2) + \lambda_6 A^2 B^2 = 0, \\ &\lambda_4 (f_0 A^2 B^2 + f_1 f_2 P_3 A^2 B - f_1^2 f_2 P_1 P_3 A^2) \\ &- \lambda_5 f_1^2 f_2 P_2 P_3 B^2 - \lambda_6 A^2 B^2 = 0, \\ &\lambda_4 (f_1 f_2 P_1 A^2 B - 4 f_1 f_2^2 P_1 P_3 A^2) - \lambda_6 A^2 B^2 \\ &+ \lambda_5 (f_1 f_2 P_2 A B^2 - 4 f_1^2 f_2 P_2 P_3 B^2) = 0, \\ &\lambda_4 + \lambda_5 = 1, \\ &P_1 + P_2 + P_3 = P_T, \\ &(f_0 P_1 - f_0 P_2) A B + f_1 f_2 P_3 (P_1 A - P_2 B) = 0. \end{aligned} \tag{23}$$

where $A = 4 f_1 P_3 + f_1 P_1 + f_2 P_2 + 2$ and $B = 4 f_2 P_3 + f_1 P_1 + f_2 P_2 + 2$, and we use $P_3 = P_{R_i}$ for simplicity of expression. The solutions of Eq. (23) can be calculated numerically. However, the correct solution needs to be carefully chosen due to the high order equations, then the optimal power allocation can be achieved.

Although the KKT solution is optimal, it has high computation complexity. Next, we derive a sub-optimal solution by approximating Eq. (12).

2) Approximate Solution of Eq. (12): To get a low-complexity approximate solution of Eq. (12), note that when a relay is selected in our system, the direct link must be in deep fading, *i.e.*, the received signal from the direct link is significantly degraded. Therefore, we can neglect the SNR contribution of the direct link from the MRC combined SNR in Eq. (9). Then the received SNRs at the two users become

$$\begin{aligned} SNR_{21}^{(3)} &= \frac{P_2 f_1 f_2 w_i^2}{4 f_1 w_i^2 N_0 + N_0}, \\ SNR_{12}^{(3)} &= \frac{P_1 f_2 f_1 w_i^2}{4 f_2 w_i^2 N_0 + N_0}. \end{aligned} \tag{24}$$

$SNR_{21}^{(3)} = SNR_{12}^{(3)}$ is equivalent to

$$P_2 (4 f_2 w_i^2 + 1) = P_1 (4 f_1 w_i^2 + 1). \tag{25}$$

Without loss of generality, let $N_0 = 1$, and it is obvious that the total power inequality should take equal sign to maximize the powers. Then the optimization problem in Eq. (12) can be rewritten as

$$\begin{aligned} \max_{P_i} \quad & \frac{P_1 (P_T - P_1 - P_2) f_1 f_2}{P_1 (f_1 - 4 f_2) - 3 f_2 P_2 + 4 f_2 P_T + 2} \\ s.t. \quad & 3 (f_2 P_2^2 - f_1 P_1^2) + 5 P_1 P_2 (f_2 - f_1) \\ & + 4 P_T (f_1 P_1 - f_2 P_2) + 2 (P_1 - P_2) = 0. \end{aligned} \tag{26}$$

Let the objective function be $A(P_1, P_2)$ and the equality constraint be $B(P_1, P_2)$, using Lagrange multiplier method, the Lagrangian function of Eq. (26) can be written as

$$\mathcal{L}(P_1, P_2, \lambda) = A(P_1, P_2) - \lambda B(P_1, P_2). \tag{27}$$

Solving $\nabla_{P_1, P_2, \lambda} \mathcal{L}(P_1, P_2, \lambda) = 0$, two sets of closed-form solutions for P_1 and P_2 are obtained. By eliminating the set of solution that does not satisfy the total power constraint $P_1 + P_2 + P_{R_i} \leq P_T$, the unique power allocation of P_1^*, P_2^* and $P_{R_i}^*$ can be achieved.

After power allocation, the optimal SNRs for the two users can be computed by plugging the solution of $P_1^*, P_2^*, P_{R_i}^*$ into Eq. (9). It should be noted that the obtained SNRs for the two users are not equal in that we ignore the SNR contribution from the direct link. To satisfy the data rate fairness constraint, a compensation parameter $\beta < 1$ is introduced. Suppose the obtained optimal powers are $P_2^* > P_1^*$, the final employed power for S_2 is adjusted to βP_2^*, and the corresponding power for S_1 is then $P_1^* = P_T - \beta P_2^* - P_{R_i}^*$. The value of β can be found by bisection search such that $SNR_{21}^{(3)} = SNR_{12}^{(3)}$.

3) Relay Selection in three-phase mode: After obtaining the optimal power allocation for the two users and the relay, we need to select the best relay. As $SNR_{12}^{(3)} = SNR_{21}^{(3)} = SNR_{R_i}$ is a function of channel parameters h_{1i}, h_{2i}, h_0, the relay selection problem is solved within a candidate relay set $R_i \in \mathcal{R}$, which is described as

$$\max_{R_i \in \mathcal{R}} \quad SNR_{R_i}. \tag{28}$$

Since the two users have the knowledge of all channel state information as described in Sec. III-A, the relay selection scheme can be adopted in a distributed manner. That is, any of the two users can select the optimal relay with maximized SNR by calculating the SNR_{R_i} as in Eq. (9). After that, a binary vector $\Phi = \{\phi_{R_i}, R_i \in \mathcal{R}\}, \phi_{R_i} = \{0, 1\}$ (1 indicates the relay is selected, and 0 otherwise) can be broadcasted to all relay nodes over a reliable channel by the user who starts the conversation.

Once the three-phase sum rate in Eq. (10) is found, it is compared with the two-phase sum rate in Eq. (3), and the mode with higher rate is selected for the current frame.

IV. Derivation of Symbol Error Probability

In this section, based on the modified TDBC protocol analyzed in Sec. III, the symbol error probability (SEP) of the proposed cooperative system is derived, from which the packet error rate (PER) can be obtained. The latter will be used in the next section for JSCC optimization. In this paper, BPSK modulation is assumed, so the SEP is the same as Bit Error Probability (BEP).

First, for transmission over the direct link described in Eq. (1) and Eq. (2), the instantaneous received SNRs at node S_1 and S_2 are given by

$$\begin{aligned} \gamma_{S_1}^0 &= \frac{|h_0|^2 P_2}{N_0} = \Gamma_{S_2}^0 |h_0|^2, \\ \gamma_{S_2}^0 &= \frac{|h_0|^2 P_1}{N_0} = \Gamma_{S_1}^0 |h_0|^2, \end{aligned} \tag{29}$$

where $\Gamma_{S_j}^0$ is the average SNR of the direct link at user S_i.

The SEP in this case can be computed by evaluating the conditional probability density function (PDF) $P_{b|h_0}(\gamma_{S_i}^0) = \frac{1}{2} erfc(\sqrt{\gamma_{S_i}^0})$ over the PDF of $\gamma_{S_i}^0$ [50].

$$\begin{aligned} P_e^{\mathrm{DL}} &= \int_0^\infty P_{b|h_0}(\gamma_{S_i}^0) p(\gamma_{S_i}^0) d\gamma_{S_i}^0 \\ &= \int_0^\infty \frac{1}{2} \mathrm{erfc}(\sqrt{\gamma_{S_i}^0}) p(\gamma_{S_i}^0) d\gamma_{S_i}^0, \\ &= \frac{1}{2} \left(1 - \sqrt{\frac{\Gamma_{S_j}^0}{\Gamma_{S_j}^0 + 1}} \right), \end{aligned} \tag{30}$$

where the PDF of $\gamma_{S_i}^0$ and erfc function are given by

$$\begin{aligned} p(\gamma_{S_i}^0) &= \frac{1}{\Gamma_{S_j}^0} e^{-\frac{\gamma_{S_i}^0}{\Gamma_{S_j}^0}}, \ \gamma_{S_i}^0 \geq 0, \\ \mathrm{erfc}(x) &= \frac{2}{\sqrt{\pi}} \int_x^\infty e^{-t^2} dt. \end{aligned} \tag{31}$$

As described in Sec. III-C, when the achievable sum rate of two-phase mode is higher than three-phase mode, there is no further relay transmission. In this case, the SEP of the two users S_1 and S_2 can be computed as in Eq. (30).

When the three-phase mode is used, the selected relay transmits the signal to the two users, and MRC is used to combine the received signals from the relay-to-user link and the direct link at the end-user. Since the AF protocol is used at the relay node, for user S_2, the channel to transmit the signal from $S_1 \to R_i \to S_2$ is a doubly cascaded Rayleigh fading channel, where R_i is the selected relay node. Let the SNRs of the $S_1 \to R_i$, $R_i \to S_2$ and $S_1 \to S_2$ links be $\gamma_{S_1 R_i}$, $\gamma_{R_i S_2}$ and $\gamma_{S_1 S_2}$ respectively. From [46], the corresponding received SNR at user S_2 after MRC is given by

$$\gamma_{S_2}^{\mathrm{MRC}} = \gamma_{S_1 S_2} + \frac{\gamma_{S_1 R_i} \gamma_{R_i S_2}}{\gamma_{S_1 R_i} + \gamma_{R_i S_2} + 1}, \tag{32}$$

From Sec. III-A, let $\gamma_{S_1 R_i} \sim \exp(\lambda_1)$ and $\gamma_{R_i S_2} \sim \exp(\lambda_2)$ be statistically independent exponential random variables. The SNR $\gamma_{S_1 R_i S_2}$ can be written as

$$\gamma_{S_1 R_i S_2} = \frac{\gamma_{S_1 R_i} \gamma_{R_i S_2}}{\gamma_{S_1 R_i} + \gamma_{R_i S_2} + 1}. \tag{33}$$

Let $Z = \gamma_{S1 R_i S_2}$. From [51], the PDF of Z is given by

$$\begin{aligned} p_Z(z) = 2e^{-(\lambda_1+\lambda_2)z} [\lambda_1 \lambda_2 (2z+1) K_0(2\sqrt{\lambda_1 \lambda_2 z(z+1)}) \\ + (\lambda_1 + \lambda_2) \sqrt{\lambda_1 \lambda_2 z(z+1)} K_1(2\sqrt{\lambda_1 \lambda_2 z(z+1)})], \end{aligned} \tag{34}$$

where K_i is the i-th order modified Bessel function of the second kind [51].

From [52], the moment-generating function (MGF) of Z, which is defined as $\mathcal{M}_Z(s) = E\{e^{-sZ}\}$, is given by Eq. (37) at the top of next page, where

$$\varphi_{\lambda_1,\lambda_2}^+(s) = \frac{1}{2} \left[s + \lambda_1 + \lambda_2 \pm \sqrt{(s+\lambda_1+\lambda_2)^2 - 4\lambda_1\lambda_2} \right] \tag{35}$$

and $\Psi(a, b; z)$ is Tricomi's confluent hypergeometric function [51].

Using the MGF-based approach in [53] and from the fact that $\gamma_{S_1 S_2}$ and $\gamma_{S_1 R_i S_2}$ are independent, the average SEP of BPSK modulation for the received MRC signal is given by

$$P_e^{\mathrm{MRC}} = \frac{1}{\pi} \int_0^\Theta \left(1 + \frac{g \Gamma_{S_1}^0}{\sin^2 \theta} \right)^{-1} \mathcal{M}_Z(\frac{g}{\sin^2 \theta}) d\theta, \tag{36}$$

$$\begin{aligned}\mathcal{M}_Z(s) = &\frac{\lambda_1+\lambda_2}{\varphi^+_{\lambda_1,\lambda_2}(s)-\varphi^-_{\lambda_1,\lambda_2}(s)}\left[\Psi\left(1,0;\varphi^-_{\lambda_1,\lambda_2}(s)\right)-\Psi\left(1,0;\varphi^+_{\lambda_1,\lambda_2}(s)\right)\right]\left(1+\frac{\varphi^+_{\lambda_1,\lambda_2}(s)+\varphi^-_{\lambda_1,\lambda_2}(s)}{[\varphi^+_{\lambda_1,\lambda_2}(s)-\varphi^-_{\lambda_1,\lambda_2}(s)]^2}\right)\\ &+\frac{\lambda_1\lambda_2}{\varphi^+_{\lambda_1,\lambda_2}(s)-\varphi^-_{\lambda_1,\lambda_2}(s)}\left[\Psi\left(1,1;\varphi^-_{\lambda_1,\lambda_2}(s)\right)-\Psi\left(1,1;\varphi^+_{\lambda_1,\lambda_2}(s)\right)\right]\left(1+\frac{\varphi^+_{\lambda_1,\lambda_2}(s)+\varphi^-_{\lambda_1,\lambda_2}(s)}{\frac{1}{2}[\varphi^+_{\lambda_1,\lambda_2}(s)-\varphi^-_{\lambda_1,\lambda_2}(s)]^2}\right)\\ &-(\lambda_1+\lambda_2)\left[\varphi^+_{\lambda_1,\lambda_2}(s)-\varphi^-_{\lambda_1,\lambda_2}(s)\right]^{-2}\left[\varphi^-_{\lambda_1,\lambda_2}(s)\Psi\left(2,1;\varphi^-_{\lambda_1,\lambda_2}(s)\right)+\varphi^+_{\lambda_1,\lambda_2}(s)\Psi\left(2,1;\varphi^+_{\lambda_1,\lambda_2}(s)\right)\right]\\ &-2\lambda_1\lambda_2\left[\varphi^+_{\lambda_1,\lambda_2}(s)-\varphi^-_{\lambda_1,\lambda_2}(s)\right]^{-2}\left[\varphi^-_{\lambda_1,\lambda_2}(s)\Psi\left(2,2;\varphi^-_{\lambda_1,\lambda_2}(s)\right)+\varphi^+_{\lambda_1,\lambda_2}(s)\Psi\left(2,2;\varphi^+_{\lambda_1,\lambda_2}(s)\right)\right]\end{aligned} \tag{37}$$

where $\Theta=\pi/2$ and $g=\sin^2(\pi/2)$ for BPSK modulation.

As discussed before, there are two possible transmission modes in the proposed scheme, depending on the achievable sum rate of the two cases. Let $\mathcal{C}_i \in \mathcal{A}$ denote case i, and $\mathcal{A}=\{2\text{-phase}, 3\text{-phase}\}$ is the set of all cases. The average SEP for S_2 can be expressed as

$$\Pr\{\varepsilon\} = \sum_{\mathcal{C}_i\in\mathcal{A}} P_e\{\mathcal{C}_i\}\Pr\{\varepsilon|\mathcal{C}_i\}. \tag{38}$$

Plugging Eqs. (30) and (36) into Eq. (38), the average SEP of the proposed system can be obtained. It should be noted that the $\Pr\{\varepsilon|\mathcal{C}_i\}$ in Eq. (38) depends on the comparison of the achievable sum rates between two-phase and three-phase transmissions, which can be obtained by simulations in certain network setup.

V. Joint Source-channel Coding for JPEG 2000 Codestream Transmission

In this section, a JSCC scheme is formulated and solved for error-resilient (ER) transmission of JPEG 2000 bitstream over the proposed two-way relay system. The overall goal is to maximize the reconstructed image quality under a total rate constraint. To achieve this, we need to determine the number of transmitted JPEG 2000 layers and the level of channel coding protection. The scheme also takes full advantage of the ER tools in the JPEG 2000 standard.

A. Error-Resilient Tools of JPEG 2000

When encoding an image, the JPEG 2000 encoder first divides the image into disjoint rectangular tiles. Multiple levels of DWT are then applied to each tile to generate various subbands. Each subband is further divided into rectangular precincts, and each precinct is composed of some codeblocks. The codeblock is the basic coding unit. The bitplane-based embedded entropy coding in JPEG 2000 is applied to each codeblock. After that, a truncation algorithm is employed to collect the outputs of coding passes from different codeblocks to form different quality layers of the codestream [2].

JPEG 2000 also provides several ER tools [2] to maximize the decoded quality when error occurs in the codestream. The ER tools can be classified into three types: resynchronization for packet protection, segmentation for codeblock protection and error resilient termination for codeblock protection [2]. As introduced above, in JPEG 2000, the codeblock is the basic independent coding unit. The errors will not propagate from one codeblock to another as long as the codeblock resynchronization is maintained. With the correct packet header information, the JPEG 2000 decoder is able to identify the length of bytes for each codeblock. Hence, even though there exist errors in the data of one codeblock, the decoder can maintain synchronization for other codeblocks.

Besides the resynchronization protection and segmentation for codeblock protection, JPEG 2000 also provides several mechanisms to enhance the reconstructed quality within a single codeblock. Some related mode variations of JPEG 2000 are introduced as follows. Although some of the mode variations are not designed for the purpose of error resilience, we will discuss how they can affect the error resilience.

When the RESET mode is used, the context states are reset to the default values at the beginning of each coding pass. Otherwise, the context states are initialized only once prior to the first coding pass. Although the forced reset of the context states at each coding pass reduces coding efficiency, it enables parallel implementation of coding passes. When the RESTART mode is used, the MQ coder is restarted at the beginning of each coding pass. Then, each coding pass can have its own MQ codeword segment. At the end of each coding pass, the codeword segment for that coding pass is appropriately terminated and the coder is re-initialized for the next coding pass. Note that MQ coder initialization does not reset the context states, which is controlled by RESET switch. When the ERTERM mode is used, a predictable termination policy is used by the MQ coder for each codeword segment. Then, it is possible for decoders to exploit the properties of this termination policy to detect potential errors. When the SEGMARK mode is used, a string of four binary symbols must be encoded at the end of each bit-plane. The decoder will detect these four symbols before proceeding to the next bit-plane. An error resilient implementation of the decoder may use SEGMARK symbols to detect the presence of errors and take measures to conceal the effects of these errors.

By combining these modes, various mechanisms can be achieved to enhance the error resilience. For instance, when the SEGMARK and ERTERM modes are used concurrently, with the inserted special four symbols of SEGMARK, a single error in a bit-plane is likely to be detected. The error resilient decoder will attempt to discard those coding passes that are suspected to contain errors. However, the decoder cannot distinguish which of the three coding passes contain errors, thus all of them have to be discarded. Another combination is

to use the RESTART and ERTERM modes simultaneously. In this case, a separate predictably terminated codeword segment for each coding pass is created. An error resilient decoder can detect error at the end of the coding pass, and discards only those coding passes which are affected by the error. Since RESTART and ERTERM modes can provide better error resilience than that offered by SEGMARK mode, we adopt RESTART and ERTERM modes in this paper. There are some other markers that can help locating and synchronizing the bitstream, such as start of a packet (SOP) and end of packet header (EPH), which are also used in this paper.

In Part 11 of the JPEG 2000 standard, wireless JPEG 2000 (JPWL) [54] defines techniques to increase the error resilience when transmitting codestreams over wireless network. JPWL specifies the tools such as forward error correction (FEC), interleaving and unequal error protection (UEP). Our proposed system is fully compliant with the JPWL.

B. Problem Formulation

In this paper, the JPEG 2000 codec first generates L quality layers for the whole image. The JSCC algorithm then decides how many quality layers should be included into the final output codestream and what channel codes should be allocated accordingly, based on the rate constraint. Note that when the number of quality layers is determined, the distortion reduction of each codeblock is determined correspondingly.

There are some existing JSCC methods for JPEG 2000. In [30], the proposed UEP method provides good performance by optimizing on coding pass level, but it has high complexity due to the large number of coding passes in JPEG 2000 codestream. In [34], a packet-level UEP method is proposed by using dichotomic search. However, the packet-level UEP method still has higher complexity than the method that will be developed in this paper. Further, it fails to consider the ER tools that can improve the codestream with errors. Since our objective is to design a JSCC approach for JPEG 2000 transmission over the proposed two-way multi-relay system, different from other existing JSCC methods, it requires low complexity and high robustness.

Denote D_i and N as the distortion reduction for codeblock i and the number of codeblocks in the image, respectively. Let Q be the number of quality layers included in the final codestream, where $Q \in \{1, 2, \cdots, L\}$, and L is the maximum number of generated layers for one image.

Due to the independent encoding of each codeblock, the total expected distortion reduction of the image is the sum of the expected distortion reductions of all codeblocks [2].

$$D_{Total} = \sum_{i=1}^{N} E[D_i], \tag{39}$$

where the expected distortion reduction of each codeblock will be defined in Eq. (42).

Let k_i be the number of *source coding packets* for the i-th codeblock, with the same length for each packet (this packet is different from the encoded packets of JPEG 2000 encoder, denoted as J2K packet). In addition, let n_i be the total assigned number of packets for codeblock i (including *source coding packets* and *channel coding packets*). The allocated number of *channel coding packets* is then $n_i - k_i$, and a channel coding packet has the same length as a source coding packet. To successfully recover codeblock i, we need to correctly receive at least k_i packets from the n_i transmitted packets. Denote $\mathcal{N} = \{n_1, n_2, \cdots, n_N\}$ as the numbers of packets for all codeblocks, *i.e.*, $\mathcal{N}$ represents the rate allocation for the entire codestream and n_i is the rate allocation for codeblock i.

Define $P_{CB_i}(k_i, n_i)$ as the probability of the decoding failure of codeblock i, which can be computed as

$$P_{CB_i}(k_i, n_i) = 1 - \sum_{i=k_i}^{n_i} \binom{n_i}{i} (1 - P_{pack})^i, \tag{40}$$

where P_{pack} is the packet error rate (PER). Assume r symbols are included in a packet and the errors are uniformly distributed, then the PER is expressed as

$$P_{pack} = 1 - (1 - P_s)^r, \tag{41}$$

where P_s is the SER obtained from Sec. IV.

The expected distortion reduction of a single codeblock i can then be depicted as $E[D_i]$, which is given by

$$E[D_i] = (1 - P_{CB_i}(k_i, n_i))D_i + P_{CB_i}(k_i, n_i)D_i^{ER}, \tag{42}$$

where D_i^{ER} is the decoded distortion reduction for codeblock i when less than k_i packets are successfully received. In this case, some of the coding passes are destroyed in the codeblock.

As discussed in Sec. V-A, by employing RESTART/ERTERM mode, the decoder can detect an error within a particular coding pass with high reliability. Thus, all previous coding passes can be restored rather than discarding all coding passes in this codeblock. In this way, more distortion reduction can be achieved within a single codeblock compared to encoding without ER tools. Note that if the location of the first error within a coding pass is available (this can be achieved by using some external methods, such as information from transport layer of packet-switched networks), partial decoding can be achieved even for some future coding passes within this codeblock [55]. This mechanism can be employed to our proposed method to further improve the performance. However, it is beyond the scope of this paper.

The restored distortion reduction D_i^{ER} varies depending on the location of the first error occurrence in that codeblock. Generally, this D_i^{ER} term is much smaller than D_i. Although we can estimate the distortion reduction of each coding pass, in this case, it is hard to estimate D_i^{ER} in that we cannot obtain the information of where the first error occurs in that codeblock. D_i^{ER} is related to the symbol error rate and the distortion reduction of the coding passes in that codeblock. Without loss of generality, we set it to a set of constant numbers according to the channel conditions and the resolution that codeblock belongs to, since the codeblocks in the same resolution usually have similar distortion reduction. We have conducted simulations to obtain the D_i^{ER} of different images under different network conditions and resolutions. Discussions will be made in Sec. VI-C to find the regularity of D_i^{ER}.

The total expected distortion reduction of the entire codestream is a function of both Q and $\mathcal{N}$, which determine the

number of source coding packets and the number of channel coding packets, respectively.

As discussed in Sec. V-A, each codeblock is encoded independently, and the significance of the codeblock decreases along the codestream [2]. In other words, the codeblocks of lower resolutions generally contribute more distortion reductions. Intuitively, we should allocate stronger channel codes to the codeblocks of lower resolutions. In this case, it is reasonable to assume that if codeblock i cannot be decoded correctly, it is very likely that codeblock $i+1$ cannot be decoded either.

The optimization problem can be formulated as

$$\begin{aligned} &\max_{\mathcal{N},Q} E[D_{Total}] = \sum_{i=1}^{N} E[D_i(\mathcal{N})] \\ &s.t. \quad \sum_{i=1}^{N} n_i \le n_{Total}, \end{aligned} \tag{43}$$

where n_{Total} is the maximum number of packets that can be included in the final JSCC codestream.

The total expected distortion reduction in Eq. (43) is expressed as the summation of expected distortion reductions of individual codeblocks, which are

$$\begin{aligned} E[D_i(\mathcal{N})] &= \prod_{j=1}^{i} (1 - P_{CB_j}) D_i \\ &+ \prod_{j=1}^{i-1} (1 - P_{CB_j}) P_{CB_i} D_i^{ER}, \quad i = 1, \cdots, N. \end{aligned} \tag{44}$$

where D_i^{ER} is the distortion reduction provided by ER tools as described above, and $P_{CB_0} = 0$.

C. Solutions to the JSCC Optimization

Eq. (43) is a discrete combinatorial optimization problem, which is difficult to solve directly, as it is not convex and we need to jointly optimize the two parameters $\mathcal{N}$ and Q. The general solution is to use Lagrangian multiplier method to solve this problem, which can be written as

$$\begin{aligned} &\max_{\mathcal{N},Q} \left\{ \sum_{i=1}^{N} E[D_i(\mathcal{N})] + \lambda (\sum_{i=1}^{N} n_i) \right\} \\ &= \max_{\mathcal{N},Q} \left\{ \sum_{i=1}^{N} (E[D_i(\mathcal{N})] + \lambda n_i) \right\} \end{aligned} \tag{45}$$

where the second step is due to the fact that each codeblock is encoded independently. The optimization can be divided into two parts. The first part is the optimization of the Lagrangian multiplier λ, which can be solved by numerical method or bisection search. The second part is the individual optimization for each codeblock to determine the optimal channel codes. The two parts need to be optimized jointly.

Although the Lagrangian multiplier method can be applied to solve Eq. (43), it is not the most efficient method in our case. The reason is that our aim is to design a real-time and error resilient image/video transmission framework over two-way multi-relay networks, which requires low complexity. One of our optimization granularity is the quality layer, which is limited in our setup (usually less than 15 layers). To reduce the complexity, instead of using the Lagrangian multiplier method, we optimize the two parameters iteratively until convergence. It should be noted that if the number of quality layer is large, the Lagrangian multiplier method can be more efficient than the proposed iterative method.

The procedure of our optimization method is as follows. First, we assume $\mathcal{N}$ in Eq. (43) is fixed, then we try to find the optimal Q. That is, we try to find the optimal number of quality layer that should be included into the final output under the allocated channel codes for all codeblocks. Note that when the number of quality layer is determined, the corresponding number of source packet for each codeblock is also determined.

A local search for Q within a small range is employed to try to increase the value of the objective function in Eq. (43) under the rate constraint. That is, we fix the total number of packets (source coding packets plus channel coding packets) allocated for all codeblocks, and adjust the number of source coding packets by tuning the Q parameter. Since the number of quality layers is limited, this step converges very fast.

Next, three methods are proposed to find the optimal $\mathcal{N}$ when Q is fixed. The first approach is the naive exhaustive search, which can find the optimal $\mathcal{N}$, but has very high complexity, and is only used as the ground truth. The second method is based on backward dynamic programming, which yields lower computation complexity. The third method employs the branch and bound algorithm by using some predefined naive JSCC strategies to further reduce the complexity of dynamic programming approach.

1) Exhaustive Search (ES): By enumerating all possible $\mathcal{N}$ and substituting into Eq. (43), the optimal scheme $\mathcal{N}^*$ can be obtained. Let r_i, $i = 1, ..., C$ be the increasing order of available channel code rates for each codeblock. r_i can be converted into packet-level FEC rate by the ratio of source and channel packets. The search space for $\mathcal{N}$ is thus C^N, which is usually too large to be searched directly in practice.

2) Dynamic Programming (DP): To reduce the complexity, we next present a dynamic programming method. The key idea is to divide the problem in Eq. (43) into several sub-problems, which can be solved stage by stage. As each codeblock is encoded independently, it is reasonable to divide the total expected distortion formula into stages of various codeblocks.

The total expected distortion reduction is given in Eq. (44). We first divide it into several stages. Given a rate allocation scheme $\mathcal{N}$, let $\Delta(i, \mathcal{N})$ be the distortion reduction from codeblocks i to N given that the first $i-1$ codeblocks are all correctly decoded. $\Delta(i, \mathcal{N})$ can be expressed as

$$\Delta(i, \mathcal{N}) = (1 - P_{CB_i}) [D_i + \Delta(i+1, \mathcal{N})] + P_{CB_i} D_i^{ER}. \tag{46}$$

By using this recursive formula, for each codeblock, Eq. (46) is the corresponding stage that needs to be maximized. The optimal n_i that maximizes Eq. (46) can be obtained by searching for all possible n_i for codeblock i.

As there are k_i source coding packets for codeblock i, codeblock i must transmit at least k_i packets and no more

than k_i/r_1 total packets (with the strongest channel code protection). It also needs to satisfy the constraint in Eq. (43).

Thus, the maximized $\Delta^*(i,\mathcal{N})$ can be expressed as

$$\Delta^*(i,\mathcal{N}) = \max_{n_i \in \{k_i,\cdots,n_i^{\max}\}} \Delta(i,\mathcal{N}), \tag{47}$$

where $n_i^{\max} = \min\{k_i/r_1, n_{Total} - l_i\}$ is the maximum total packets that can be included in codeblock i, and l_i denotes the total packets allocated to the first $i-1$ codeblocks. Similar to ES, the search space of n_i is also limited by the available converted channel codes from r_i.

The proposed DP method starts from the last codeblock N and processes backward to the first one. For each codeblock, the method computes the maximal value of Eq. (47) for each possible n_i. The backward path that leads to the maximal initial call $\Delta(1,\mathcal{N})$ gives the optimal solution to Eq. (43).

The complexity of Eq. (47) is related to the searching space of current stage and the parameter l_i. Assume the possible number of l_i is $|l_i|$, without any code constraint, the complexity of the DP optimization is $O(\sum_{i=1}^{N}(|l_i|C))$. The result of each stage is stored to prevent repeated computation.

3) DP with Branch and Bound (DP+BB): Given fixed Q, although the DP algorithm can greatly reduce the complexity compared to the exhaustive search, it can still be improved. As for codeblock i, some searching branches, *i.e.*, the candidate n_i for codeblock i, may not lead to the optimal solution, which can be ignored to further reduce the computation complexity.

Inspired by [56], we use the BB method to further limit the DP search space, i.e., before enumerating the candidates of n_i for codeblock i, the searching branch is compared with certain pre-defined solution, and the branch is discarded if it cannot provide a better solution than the best one found so far.

We first compute the objective function in Eq. (43) for a simple selection of $\mathcal{N}$, e.g., equal error protection (EEP) where the channel code rate employed for each codeblock is the same. Denote its objective value as D_{EEP}. We can also use some UEP schemes as the pre-defined solutions, which can yield even lower complexity. Without loss of generality, only EEP is used as pre-defined solution in this paper.

When Eq. (47) is called, for each possible n_i, an upper bound $\Delta^{upper}(i,\mathcal{N})$ is first derived, which is the supreme limit of the distortion reduction given that n_i is chosen for codeblock i. $\Delta_i^{upper}(i,\mathcal{N})$ can be computed by the same formula as in Eqs. (46) and (47). Further, as n_i packets are allocated to the codeblock i, when it comes to codeblock $i+1$, there are total $\sum_{j=1}^{i} n_j$ packets allocated to the first i codeblocks. To obtain an upper bound for codeblock i with total packets number n_i, we ignore the n_i packets that are allocated for codeblock i. That is, we assume $\sum_{j=1}^{i-1} n_j$ packets are allocated for the first i codeblocks, and n_i packets that are intended to be allocated to codeblock i remain in the budget to be allocated for latter codeblocks. Note that, in this way, the obtained JSCC allocation scheme $\mathcal{N}$ may not satisfy the system constraint in Eq. (43). After the upper bound $\Delta^{upper}(i,\mathcal{N})$ is obtained, if $\Delta^{upper}(i,\mathcal{N}) < D_{EEP}$, then there is no need to further compute $\Delta^{upper}(i+1,\mathcal{N})$ as it cannot provide a better solution than our pre-defined solution. Thus, more computation complexity is reduced by using the obtained upper bound.

It is shown in [30] that the optimal strength of the channel code decreases along the JPEG 2000 codestream, thanks to the embedded property. That is, the optimal protection levels for codeblocks decrease in our case in general. It implies that the search space of channel codes for codeblock $i+1$ is less than codeblock i. The can be applied to the proposed DP algorithm to further reduce the complexity.

VI. Experimental Results

A. Experimental Setup

In this section, we first show the performance of the adaptive TDBC protocol with fairness constraint in Sec. III-C. Next, the performance of the proposed JSCC method in Sec. V is evaluated, which is denoted as *JSCC-Proposed*. Then we compare our combined JSCC and two-way multi-relay scheme with other schemes.

All simulations are tested with the OpenJPEG implementation of the JPEG 2000 standard. Five-level (9,7) wavelet transform decomposition, 64×64 codeblock size, ERT-ERM+RESTART modes, 12 quality layers, SOP, and EPH markers are used. Since the SOP and EPH markers are critical for reconstruction, we allocate the strongest channel codes for them to ensure they can be decoded correctly in all cases. The packet size of source packet and channel packet is set to 50 bytes, and zero padding is applied when needed.

B. Adaptive TDBC Protocol with Fairness Constraint

In this section, the performance of the joint optimization for the adaptive TDBC protocol is compared to other conventional schemes. In this simulation, 10 candidate relays are employed. All channels are generated as zero mean normal complex random variables with unit variance, and we set $N_0 = 1$.

Fig. 3 shows the comparison of the average maximum achievable rate of each user of four schemes: the proposed KKT scheme in Sec. III-C1, the proposed approximation scheme in Sec. III-C2, optimal relay selection with equal power allocation (ORS+EPA), and random relay selection with equal power allocation (RRS+EPA). Note that, the curve of the proposed KKT and approximation schemes are half of the rates to the solutions to Eq. (11). For the two EPA schemes, the total power P_T is equally allocated to the two users and the selected relay according to the 3-phase or 2-phase case. For ORS+EPA scheme, the average rate of the two users is defined as $\max\{R^{(2)}, R^{(3)}\}$, which is the higher rate of the 2-phase and 3-phase cases. Since the two users' rates are unbalanced for the 3-phase case with EPA, we set it to $R^{(3)} = \frac{1}{3}\log_2(1 + \max_{R_i} \min(SNR_{12}^i, SNR_{21}^i))$, and

$$\begin{aligned} SNR_{21}^i &= \frac{f_1 f_2 P_T^2}{3(5f_1P_T + f_2P_T + 6)} + \frac{1}{3}P_T f_0, \\ SNR_{12}^i &= \frac{f_1 f_2 P_T^2}{3(5f_2P_T + f_1P_T + 6)} + \frac{1}{3}P_T f_0, \end{aligned} \tag{48}$$

where f_0, f_1, f_2 are defined in Sec. III-C. For RRS+EPA scheme, the only difference from ORS+EPA scheme is that the rate for 3-phase case is set to $R^{(3)} = \frac{1}{3}\log_2(1 + \min(SNR_{12}^i, SNR_{21}^i))$, and the relay R_i is selected randomly.

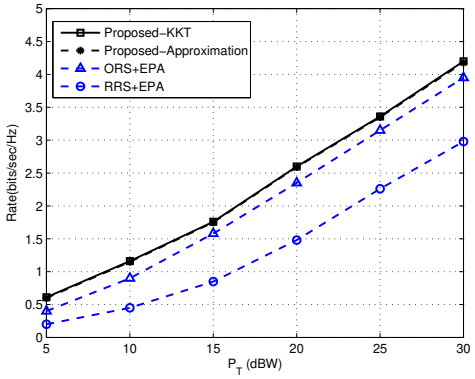

Fig. 3. Average rates vs. P_T with ten relays.

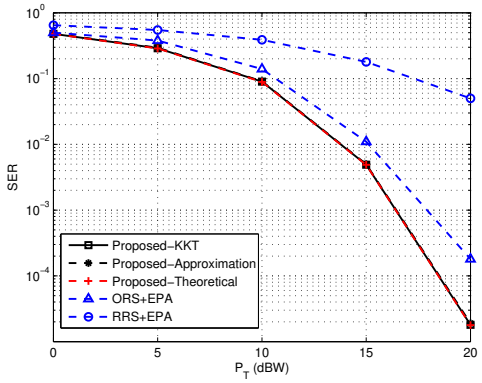

Fig. 4. Average SERs vs. P_T with ten relays.

It is obvious that relay selection has more impact on the rate performance than power allocation. However, without power allocation, one user may have a much higher rate than the other one, which makes the two users' transmission unbalanced. The proposed power allocation adjusts the two users' powers to make them having the same transmission rate. Our proposed schemes outperform the two reference schemes with average 0.272 bits/sec/Hz and 1.094 bits/sec/Hz.

Fig. 4 shows the comparison of the average symbol error rates (SERs) of our proposed schemes and other two EPA schemes, and the derived theoretical SER is also plotted. Our proposed schemes achieve the best performance, especially compared to the RRS+EPA scheme, which is mainly caused by the diversity loss of RRS. The KKT and approximation schemes are close to the theoretical curve with error less than 1%. Combined the simulation results in terms of rate and SER, our proposed scheme provides better performance than other conventional schemes.

C. Performance of the Proposed JSCC Method

In this part, the effectiveness of the proposed JSCC method is compared with EEP method and three other UEP methods in [29], [30], [34]. Meanwhile, we also conduct simulations to show how the D_i^{ER} parameter in Eq. (42) is estimated for different cases and how it affects the final optimized results.

Reed-Solomon code is chosen as the channel code for FEC protection, and 6 code rates $\{1, 0.8, 0.6, 0.5, 0.3, 0.1\}$ are available, where rate 1 has no channel coding. Every 400 codestream bits are encoded by the channel coding. Lenna (512×512), Man (1024×1024) and Airport (1024×1024) are used as test images in this experiment.

TABLE I
COMPARISON OF TIME CONSUMPTION (TC) AND PSNR BETWEEN OUR PROPOSED JSCC AND [30]

	Proposed		[30]	
	PSNR (dB)	TC (sec)	PSNR (dB)	TC (sec)
Lenna	37.78	2.39	37.75	8.58
	36.20	0.43	36.26	5.74
Man	35.92	1.89	35.79	5.51
	34.89	0.40	34.92	3.92
Airport	33.60	1.96	33.54	6.25
	32.26	0.34	32.30	4.78
Goldhill	36.03	2.14	36.01	4.21
	34.88	0.31	34.93	3.16

First, our proposed JSCC method is compared with other schemes over Rayleigh fading channel (direct link). The total rate constraint is set to 0.5 bpp, and each simulation is obtained by averaging 100 trials. The results are presented in Fig. 5. The schemes in [29], [30], [34] are denoted as Stankovic03, Wu05, and Baruffa06, respectively, and equal power allocation (EEP) scheme is also presented.

It can be seen from these figures that [30] has the best performance, due to the coding-pass-level optimization it utilizes. Our proposed method is on average 0.2-0.3 dB lower in PSNR than [30], but outperforms other schemes. However, since our method uses codeblock-level optimization, it has lower complexity than [30], especially at low PSNRs. To further illustrate this, Table I compares the time consumptions of the two methods for four images with total bit rate of 1 bpp and SNR of 16 dB in the direct link. Two PSNRs are tested for each image. To get fair comparison, we make the PSNRs of the two methods as close as possible, by adjusting the number of quality layers in our method and the number of coding passes in [30]. Each result is obtained by averaging 100 trials. It can be observed that for the higher PSNR example in each image, the speed of our method is about 2-4 times as fast as that of [30], whereas for the lower PSNR example, our method is about 10-14 times as fast as [30], making our method more suitable for real-time applications.

Next, the performances of the ES, DP and DP+BB schemes in Sec. V are compared. As ES is the optimal solution to Eq. (43), we take it as the ground truth. In order to perform ES, we reduce the number of channel code rates from 6 to 4, $\{1, 0.8, 0.5, 0.3\}$, otherwise the solution space will be too large to search directly. The various schemes are performed under total rate constraints of 0.10, 0.25, 0.50 and 1 bpp, respectively. For each rate, the results are obtained by averaging 100 trials. Table II shows the performance comparisons of ES, DP and DP+BB schemes under the average channel SNR of 15 dB for Lenna and Man images. It can be seen that ES achieves the best performance as expected. The DP approach achieves similar performance to ES scheme, and the PSNR gap is usually less than 0.3 dB. DP+BB has about 0.1-0.2 dB PSNR loss compared to DP scheme due to the reduced complexity.

Table III compares the complexities of different schemes in terms of time consumption (second), including ES, DP

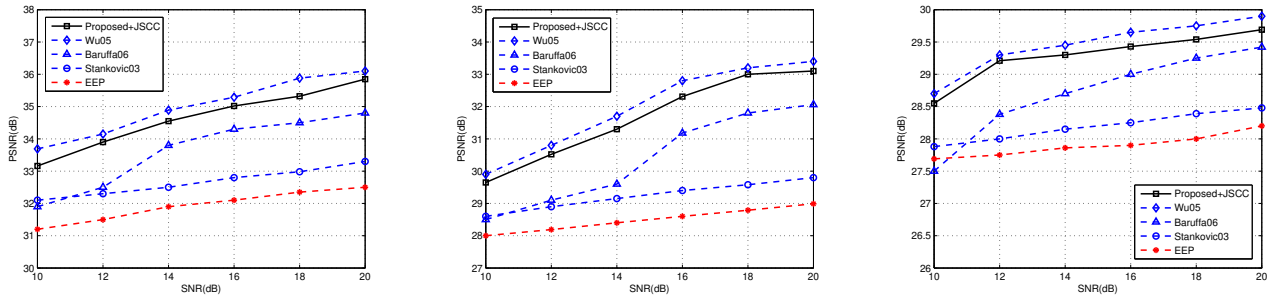

(a) Lenna (b) Man (c) Airport

Fig. 5. JSCC performance comparison with other schemes under the direct link transmission.

and DP+BB in Sec. V. The total rate is set to 0.5 bpp. The average SNR of the channel is 15 dB, and 4 channel code rates are available: $\{1, 0.8, 0.5, 0.3\}$. Each result is obtained by averaging 100 trials. It can be seen that DP and DP+BB are much faster than ES. Especially, the DP+BB method is able to optimize within 1 second. By reducing the number of quality layers, even lower time consumption can be expected.

As discussed in Sec. V-B, the D_i^{ER} parameter is related to the symbol error rate (SER) and the resolution that codeblock belongs to. Since the distortion reductions of the codeblocks within the same resolution are similar, we set the D_i^{ER} of the same resolution to a constant number for simplicity. We conduct simulations to show the results of the obtained D_i^{ER} for different images under various conditions, which are shown in Table IV in terms of MSE. Without loss of generality, lossless encoding is employed, each D_i^{ER} is obtained by averaging 100 trials. It should be noted that the $\bar{D}_{Res}^i$ parameter is the average error-free encoded distortion reduction of one codeblock of that resolution, which can be obtained from the encoder and is used as a comparison benchmark. We can observe that as the SER increases, the D_i^{ER} decreases significantly, which agrees with our analysis. Higher resolution has smaller D_i^{ER} than lower resolution because the lower resolution has more significant data. When multiple quality layers are generated, we can obtain the D_i^{ER} similarly.

Under the same SER, the D_i^{ER} of different images within the same resolution varies greatly. Therefore, it is not reasonable to allocate the same value of D_i^{ER} to all images. However, since the D_i^{ER} is related to the SER and the resolution that codeblock belongs to, it is intuitive to assume that the D_i^{ER} can be approximately written as a function of the SER and $\bar{D}_{Res}^i$ as follows.

$$D_i^{ER} \doteq \bar{D}_{Res}^i \cdot (\alpha P_s + \beta), \tag{49}$$

where α and β are constant parameters that can be obtained by least squares method, P_s is the SER that can be obtained from Sec. IV. In this way, the D_i^{ER} parameter can be estimated for various scenarios easily. Though we can use higher order function to obtain more accurate relationship in Eq. (49), it requires higher complexity as well, and the improvement to the overall performance is limited. Therefore, we use one dimensional model to estimate the relationship in Eq. (49).

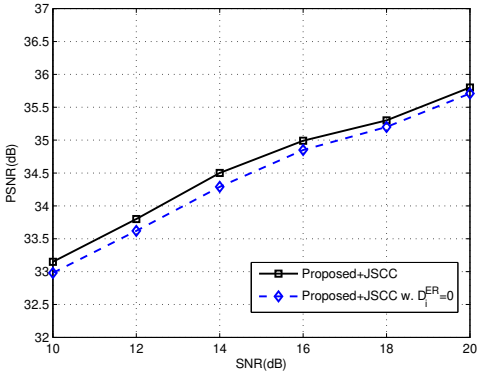

Fig. 6. Comparison of performance improvement of estimated D_i^{ER} with $D_i^{ER} = 0$ for Lenna.

TABLE II
COMPARISON OF ES, DP AND DP+BB

	Bit Rate (bpp)	0.1	0.25	0.50	1.0
Lenna	ES (dB)	29.17	32.25	35.14	37.13
	DP (dB)	29.08	31.95	35.02	37.04
	DP+BB (dB)	29.01	31.88	34.83	36.87
Man	ES (dB)	27.48	29.95	32.26	35.17
	DP (dB)	27.39	29.85	32.17	34.86
	DP+BB (dB)	27.20	29.65	32.01	34.63

We also conduct simulation to show the performance improvement provided by the estimated D_i^{ER} in Eq. (49). Without loss of generality, we set $D_i^{ER} = 0$ and compare the performance of the corresponding optimization with the case under our estimated D_i^{ER}. Note that, if ER tools are not employed, then it is true that $D_i^{ER} = 0$. The comparison of performance of Lenna is shown in Fig. 6 in terms of PSNR. The results show that 0.1-0.2 dB gain can be achieved by using the estimated D_i^{ER} on average.

As discussed in Sec. V-C, we use iterative method to optimize the objective function rather than the conventional

TABLE III
TIME CONSUMPTIONS (SECOND) OF ES, DP AND DP+BB

Lenna			Man		
ES	DP	BB	ES	DP	BB
21.73	1.65	0.42	48.33	2.81	0.49

TABLE IV
THE RESULTS OF D_i^{ER} FOR DIFFERENT IMAGES UNDER VARIOUS CONDITIONS

	Resolution	Symbol Error Rate			$\bar{D}^i_{Res}$
		0.3	0.1	0.05	
Lenna	1	3.0971×10^7	5.7053×10^7	1.0107×10^8	2.5746×10^8
	2	3.6469×10^6	7.7025×10^6	1.2550×10^7	3.1197×10^7
	3	1.9265×10^6	4.2773×10^6	5.3474×10^6	1.4780×10^7
	4	7.9662×10^5	1.8961×10^5	2.7070×10^6	6.5137×10^6
	5	1.3112×10^5	2.3038×10^5	3.6898×10^5	1.0244×10^6
	6	1.3651×10^4	2.7622×10^4	4.6595×10^4	1.1018×10^5
Airport	1	1.4521×10^8	3.6576×10^8	5.8785×10^8	1.2749×10^9
	2	6.5015×10^6	1.4020×10^7	1.7717×10^7	5.0635×10^7
	3	6.0205×10^6	1.2304×10^7	2.3637×10^7	5.4502×10^7
	4	1.6030×10^6	3.5635×10^6	5.8013×10^6	1.3140×10^7
	5	2.8617×10^5	5.3013×10^5	8.5852×10^5	2.1647×10^6
	6	4.4363×10^4	8.9865×10^4	1.5806×10^5	3.7950×10^5
Man	1	2.7448×10^8	5.9109×10^8	8.7807×10^8	2.1941×10^9
	2	1.1286×10^6	2.2546×10^7	4.1141×10^7	9.2744×10^7
	3	5.5807×10^6	9.7418×10^6	1.6368×10^7	4.6701×10^7
	4	1.2160×10^6	2.2778×10^6	3.9400×10^6	1.0210×10^7
	5	1.8165×10^5	3.4404×10^5	5.5560×10^5	1.4170×10^6
	6	2.3539×10^4	5.0524×10^4	8.2740×10^4	1.8038×10^5

TABLE V
TIME CONSUMPTION AND PSNR COMPARISONS BETWEEN THE PROPOSED METHOD AND LAGRANGIAN METHOD

	Time consumption (sec)			PSNR (dB)		
Number of QL	10	15	30	10	15	30
Proposed	0.63	1.05	2.59	37.11	37.59	37.68
Lagrangian	1.02	1.51	2.06	37.08	37.61	37.73

Lagrangian method. The reason is that the number of quality layers in our setup is limited, and our proposed iterative method is more efficient compared to the Lagrangian method in this case. Therefore, we conduct simulations to compare the performance between the proposed iterative method and the conventional Lagrangian method. Note that the procedure of the Lagrangian multiplier method is described in Sec. V-C, and bisection method is used to find the optimal λ. We adopt the simulations under different number of quality layers, which are 10 layers, 15 layers and 30 layers. The total rate constraint is set to 1 bpp. The average SNR of the channel is set to 15 dB, and 4 channel code rates are available: $\{1, 0.8, 0.5, 0.3\}$. The performance is measured in terms of time consumption and PSNR. The results are shown in Table V. It can be observed that when the number of quality layers is limited (less than 15), our proposed iterative method is faster, and both methods achieve similar PSNRs. For the case of 30 quality layers, our proposed method spends more time. It can be expected that as the number of quality layer increases, the gap between the time consumption of the two methods will increase as well.

D. Performance Evaluation of JSCC Combined with the Proposed System

In this section, the JPEG 2000 codestream generated by the proposed JSCC scheme is transmitted over the proposed system with joint optimization. The advantages are: firstly, it is able to achieve higher data rate due to the modified TDBC protocol; secondly, the joint optimization for the proposed system maximizes the achievable rate under data rate fairness constraint, and it guarantees that the two users achieve the same performance.

For system setup, the number of relay nodes is set to 10. Simulations are conducted to compare our work with [43]. In [43], R-DSTC is used to transmit over all relay nodes, so we assume the powers are equally allocated among all relay nodes, and there is no direct link in their systems. To achieve fair comparison, two experiments are conducted in this section.

Firstly, we disable the direct link in our proposed system. This leads to the following two-phase scheme:

1) In phase 1, two users S_1 and S_2 transmit their signals to all relay nodes simultaneously.
2) Then, joint power allocation and relay selection is employed. The optimization is similar to Sec. III-C. The only difference is that the direct link is not considered.
3) In phase 2, the selected relay broadcasts the combined signal back to the two users.

Secondly, we add the direct link transmission to [43]. It is reasonable to use MRC to combine the received signals from the direct link and the R-DSTC, which is expected to further improve the performance in their proposed systems.

Though in [43], the authors use average rate as performance metric, it is easy and fair to transform the average rate to PSNR metric. JPEG 2000 coder is employed as the source coder in [43]. The results for Lenna, Man and Airport images with total rate constraint of 0.5 bpp are presented in Fig. 7. Each point in the figures is obtained by averaging 100 trials.

In the two-phase setup, our proposed scheme and [43] achieve similar performances. In the three-phase setup, our proposed scheme is about 1 dB better on average. The gain comes from the joint optimization of our proposed system and the JSCC scheme. Note that, the joint optimization in Sec. III-C ensures that the two users achieve the maximal data rate under data rate fairness constraint by choosing 2-phase or 3-phase transmission automatically. The results show that it is a good approach to optimize the JPEG 2000 transmission over two-way multi-relay network in both transmission system

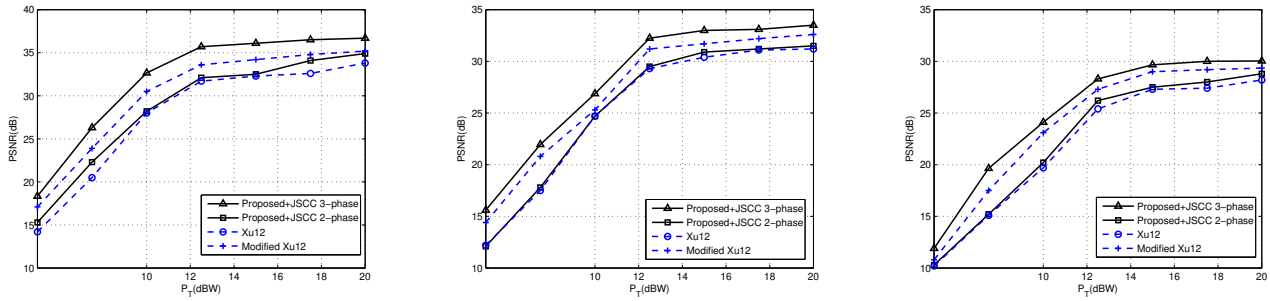

(a) Lenna (b) Man (c) Airport

Fig. 7. Performance evaluation of JSCC combined with the proposed system.

optimization and JSCC optimization. Although each method itself may not be the optimal solution compared to other methods, the low complexity and the combination of these two methods provide good performance.

VII. Conclusion

In this paper, a two-way multi-relay transmission system is proposed, which uses an adaptive TDBC protocol with optimal mode selection, relay selection and power allocation under the data rate fairness constraint. Further, a low-complexity JSCC scheme is presented to optimize the transmission of progressive error-resilient JPEG 2000 bit streams over our proposed system. We then combine the proposed JSCC and the proposed cooperative transmission system, and simulation results show that it outperforms other similar works.

Our future work includes extending the proposed two-way multi-relay framework to cognitive radio, as cognitive radio is designed to fully use the available spectrum, which is suitable for multimedia applications. Another future work is to study 3D video transmission over the proposed framework.

Acknowledgments

The authors thank the reviewers for their valuable suggestions, which have significantly enhanced the quality and presentation of the paper.

References

[1] M. Etoh and T. Yoshimura, "Advances in wireless video delivery," in *Proc. IEEE*, Jan. 2005, pp. 111–122.

[2] D. Taubman and M. Marcellin, *JPEG2000 Image Compression Fundamentals, Standards and Practice*, Kluwer Academic Publishers, 2002.

[3] ITU Recommendation, "Jpeg 2000 image coding system: Motion jpeg 2000, iso/iec final draft international stardard 15444-3," vol. T.803, Sept. 2001.

[4] L. Zheng and D. N. C. Tse, "Diversity and multiplexing: A fundamental tradeoff in multiple-antenna channels," *IEEE Trans. Inf. Theory*, vol. 49, no. 5, pp. 1073–1096, May. 2003.

[5] A. Sendonaris, E. Erkip, and B. Aazhang, "User cooperation diversity part I: System description," *IEEE Trans. Commun.*, vol. 51, no. 11, pp. 1927–1938, Nov. 2003.

[6] B. Rankov and A. Wittneben, "Spectral efficient protocols for half-duplex fading relay channels," *IEEE Journ. on Sel. Areas in Commun.*, vol. 25, no. 2, pp. 379–389, Feb. 2007.

[7] S. J. Kim, P. Mitran, and V. Tarokh, "Performance bounds for bidirectional coded cooperation protocols," *IEEE Trans. Inf. Theory*, vol. 54, no. 11, pp. 5235–5240, Nov. 2008.

[8] S. Fu, K. Lu, T. Zhang, Y. Qian, and H.-H. Chen, "Cooperative wireless networks based on physical layer network coding," *IEEE Trans. Wireless Commun.*, vol. 17, no. 6, pp. 86–95, Dec. 2010.

[9] H. Nguyen and T. Le-Ngoc, "Diversity analysis of relay selection schemes for two-way wireless relay networks," *Wireless Personal Commu.*, vol. 59, no. 2, pp. 173–189, Jul. 2011.

[10] L. Song, G. Hong, and B. Jiao, "Joint relay selection and analog network coding using differential modulation in two-way relay channels," *IEEE Trans. Veh. Technol.*, vol. 59, no. 6, pp. 2932–2939, Jul. 2010.

[11] S. Talwar, Y. Jing, and S. Shahbazpanahi, "Joint relay selection and power allocation for two-way relay networks," *IEEE Signal Process. Lett.*, vol. 18, no. 2, pp. 91–94, Feb. 2011.

[12] T. P. Do, J. S. Wang, I. Song, and Y. H. Kim, "Joint relay selection and power allocation for two-way relaying with physical layer network coding," *IEEE Commun Lett.*, vol. 17, no. 2, pp. 301–304, Feb. 2013.

[13] D. Lim, C. Chun, J. Lee, and H. Kim, "Power allocation for time division broadcast protocol over rayleigh faoding channels," in *Proc. IEEE Computing, Networking and Commu.*, San Diego, CA, Jan. 2013, pp. 133–137.

[14] G. A. S. Sidhu, F. Gao, W. Chen, and A. Nallanathan, "A joint resource allocation scheme for multiuser two-way relay networks," *IEEE Trans. Commun.*, vol. 59, no. 11, pp. 2970–2975, Nov. 2011.

[15] M. Pischella and D. L. Ruyet, "Optimal power allocation for the two-way relay channel with data rate fairness," *IEEE Commun Lett.*, vol. 15, no. 9, pp. 959–961, Sept. 2011.

[16] B. A. Banister, B. Belzer, and T. R. Fischer, "Robust image transmission using jpeg2000 and turbo-codes," *IEEE Signal Process. Lett.*, vol. 9, no. 4, pp. 117–119, Apr. 2002.

[17] V. Sanchez and M. K. Mandal, "Efficient channel protection for jpeg2000 bitstream," *IEEE Trans. Circ. Syst. Video Tech.*, vol. 14, no. 4, pp. 554–558, Apr. 2004.

[18] L. Atzori, G. Ginesu, and A. Raccis, "Jpeg2000-coded image error concealment exploiting convex sets projections," *IEEE Trans. Image Proc.*, vol. 14, no. 4, pp. 487–498, Mar. 2005.

[19] D. Taubman and J. Thie, "Optimal erasure protection for scalably compressed video streams with limited retransmission," *IEEE Trans. Image Proc.*, vol. 14, no. 8, pp. 1006–1019, Jul. 2005.

[20] R. Hamzaoui, V. Stankovic, and Zixiang Xiong, "Optimized error protection of scalable image bit streams," *IEEE Signal Process. Mag.*, vol. 22, no. 6, pp. 91–107, Dec. 2005.

[21] J. Thie and D. Taubman, "Optimal erasure protection strategy for scalably compressed data with tree-structured dependencies," *IEEE Trans. Image Proc.*, vol. 14, no. 12, pp. 2002–2011, Nov. 2005.

[22] Z. Guo, Y. Nishikawa, R. Y. Omaki, T. Onoye, and I. Shirakawa, "A low-complexity fec assignment scheme for motion jpeg2000 over wireless network," *IEEE Trans. Consumer Electronics*, vol. 52, no. 1, pp. 81–86, Feb. 2006.

[23] X. Pan, A. Cuhadar, and A. H. Banihashemi, "Combined source and cahnnel coding with jpeg2000 and rate-compatible low-density parity-check codes," *IEEE Trans. Signal Proc.*, vol. 54, no. 3, pp. 1160–1164, Mar. 2006.

[24] M. Grangetto, E. Magli, and G. Olmo, "A syntax-preserving error resilience tool for jpeg 2000 based on error correcting arithmetic coding," *IEEE Trans. Image Proc.*, vol. 15, no. 4, pp. 807–818, Apr. 2006.

[25] L. Pu, Z. Wu, A. Bilgin, M. W. Marcellin, and B. Vasic, "Ldpc-based iterative joint source-channel decoding for jpeg2000," *IEEE Trans. Image Proc.*, vol. 16, no. 2, pp. 577–581, Feb. 2007.

[26] M. Grangetto, B. Scanavino, G. Olmo, and S. Benedetto, "Iterative decoding of serially concatenated arithmetic and channel codes with jpeg 2000 applications," *IEEE Trans. Image Proc.*, vol. 16, no. 6, pp. 1557–1567, May 2007.

[27] L. Pu, M. W. Marcellin, I/ Djordjevic, B. Vasic, and A. Bilgin, "Joint source-channel rate allocation in parallel channels," *IEEE Trans. Image Proc.*, vol. 16, no. 8, pp. 2016–2022, Aug. 2007.

[28] J. Liu, D. Zhang, Y. Wang, and L. Wang, "Adaptive joint source-channel coding for motion jpeg2000 sequences transmission over unknown channels," in *Proc. 6th World Congress on Intelligent Control and Automation*, Dalian, China, Jun. 2006.

[29] V. M. Stankovic, R. Hamzaoui, Y. Charfi, and Z. Xiong, "Real-time unequal error protection algorithms for progressive image transmission," *IEEE Journ. on Sel. Areas in Commun.*, vol. 21, no. 10, pp. 1526–1535, Dec. 2003.

[30] Z. Wu, A. Bilgin, and M. W. Marcellin, "Joint source/channel coding for image transmission with jpeg2000 over memoryless channels," *IEEE Trans. Image Proc.*, vol. 14, no. 8, pp. 1020–1032, Aug. 2005.

[31] N. Thomos, N. V. Boulgouris, and M. G. Strintzis, "Optimized transmission of jpeg2000 streams over wireless channels," *IEEE Trans. Image Proc.*, vol. 15, no. 1, pp. 54–67, Jan. 2006.

[32] Max Agueh, J. Diouris, Magaye Diop, and F. Devaux, "Dynamic channel coding for efficient motion jpeg 2000 video streaming over mobile ad-hoc networks," in *Proc. Int. Conf. on Mobile Multimedia Commun.*, Nafpaktos, Greece, Aug. 2007.

[33] L. Jimenez-Rodriguez, F. Auli-Llinas, and M. W. Marcellin, "Fast rate allocation for jpeg2000 video transmission over time-varying channels," *IEEE Trans. Multimedia*, vol. 15, no. 1, pp. 15–26, Jan. 2013.

[34] G. Baruffa, P. Micati, and F. Frescura, "Error protection and interleaving for wireless transmission of jpeg2000 images and video," *IEEE Trans. Image Proc.*, vol. 18, no. 2, pp. 346–356, Feb. 2009.

[35] X. Pan, A. H. Banihashemi, and A. Cuhadar, "Progressive transmission of images over fading channels using rate-compatible ldpc codes," *IEEE Trans. Image Proc.*, vol. 15, no. 12, pp. 3627–3635, Dec. 2006.

[36] D. Gündüz and E. Erkip, "Source and channel coding for cooperative relaying," *IEEE Trans. Inf. Theory*, vol. 53, no. 10, pp. 3454–3475, Oct. 2007.

[37] J. Wang and J. Liang, "Optimization of the end-to-end distortion of a gaussian source in layered broadcast transmission," in *Proc. 25th Queen's Biennial Symposium on Communications*, Kington, Ontario, Canada, May 2010, pp. 49–54.

[38] J. Wang, J. Liang, and S. Muhaidat, "On the distortion exponents of layered broadcast transmission in multi-relay cooperative networks," *IEEE Trans. Signal Proc.*, vol. 58, no. 10, pp. 5340–5352, Oct. 2010.

[39] C. Bi and J. Liang, "Layered source-channel coding over two-way relay networks," in *Proc. IEEE Veh. Technol. Conf. Fall*, Las Vegas, USA, Sept. 2013, pp. 1–5.

[40] T. Q. Duong and H. J. Zepernick, "On the performance of roi-based image transmission using cooperative diversity," in *Proc. IEEE Int. Symp. on Wireless Commun. Syst.*, Reykjavik, 21-24 Oct. 2008, pp. 340–343.

[41] H. Shutoy, D. Gündüz, E. Erkip, and Y. Wang, "Cooperative source and channel coding for wireless multimedia communications," *IEEE Journ. on Sel. Areas in Signal Proc.*, vol. 1, no. 2, pp. 295–307, Aug. 2007.

[42] H. Kim, R. Annavajjala, P. C. Cosman, and L. B. Milstein, "Source-channel rate optimization for progressive image transmission over block fading relay channels," *IEEE Trans. Commun.*, vol. 58, no. 6, pp. 1631–1642, Jun. 2010.

[43] X. Xu, O. Alay, E. Erkip, Y. Wang, and S. Panwar, "Two-way wireless video communication using randomized cooperation, network coding and packet level fec," in *Proc. IEEE Int. Conf. on Commun.*, Ottawa, ON, Jun. 2012, pp. 7066–7070.

[44] A. J. Aljohani, S. X. Ng, R. G. Maunder, and L. Hanzo, "Joint ttcm-vlc-aided sdma for two-way relaying aided wireless video transmission," in *Proc. IEEE Veh. Technol. Conf. Fall*, Las Vegas, NV, Sept. 2013, pp. 1–5.

[45] O. Alay, P. Liu, Y. Wang, E. Erkip, and S. S. Panwar, "Cooperative layered video multicast using randomized distributed space time codes," *IEEE Trans. Multimedia*, vol. 13, no. 5, pp. 1127–1140, Oct. 2011.

[46] J. N. Laneman, D. N. C. Tse, and G. W. Wornell, "Cooperative diversity in wireless networks: efficient protocols and outage behavior," *IEEE Trans. Inf. Theory*, vol. 50, no. 12, pp. 3062–3080, Dec. 2004.

[47] Q. Li, S. H. Ting, A. Pandharipande, and Y. Han, "Adaptive two-way relaying and outage analysis," *IEEE Trans. Wireless Commun.*, vol. 8, no. 6, pp. 3288–3299, Jun. 2009.

[48] J. G. Proakis, *Digital Communications*, McGraw-Hill, New York, 3 edition, 2001.

[49] S. Boyd and L. Vandenberghe, *Convex Optimization*, Cambridge, U.K.: Cambridge Univ. Press, 2004.

[50] John G. Proakis and Masoud Salehi, *Digital Communications, 5th ed.*, McGraw-Hill Higher Education, 2008.

[51] I. S. Gradshteyn and I. M. Ryzhik, *Table of Integrals, Series, and Products, 7th ed.*, Academic Press in an imprint of Elsevier, 2007.

[52] B. Barua, H. Q. Ngo, and H. Shin, "On the sep of cooperative diversity with opportunistic relaying," *IEEE Commun Lett.*, vol. 12, no. 10, pp. 727–729, Oct. 2008.

[53] M. K. Simon and M. S. Alouini, *Digital communication over fading channels: A unified approach to performance analysis*, NewYork: John Wiley and Sons, 2000.

[54] F. Dufaux, G. Baruffa, F. Frescura, and D. Nicholson, "Jpwl - an extension of jpeg 2000 for wireless imaging," in *Proc. IEEE Int. Symp. Circ. and Syst.*, Island of Kos, May 2006, pp. 3870–3873.

[55] Z. Wu, A. Bilgin, and M. W. Marcellin, "Error resilient decoding of jpeg2000," *IEEE Trans. Circ. Syst. Video Tech.*, vol. 17, no. 12, pp. 1752–1757, Dec. 2007.

[56] T. Morin and R. Marsten, "Branch-and-bound strategies for dynamic programming," *Operations Research*, vol. 24, no. 4, pp. 611–627, Jul.-Aug. 1976.

Chongyuan Bi (S'14) received the B.E. and M.E. degrees from Xi'an Jiaotong University, China, in 2008 and 2011, respectively. He is currently working toward the Ph.D. degree at the School of Engineering Science, Simon Fraser University, Canada. His research interests include image/video coding, and multimedia communications.

Jie Liang (S'99-M'04-SM'11) received the B.E. and M.E. degrees from Xi'an Jiaotong University, China, the M.E. degree from National University of Singapore, and the Ph.D. degree from the Johns Hopkins University, USA, in 1992, 1995, 1998, and 2003, respectively. Since May 2004, he has been with the School of Engineering Science, Simon Fraser University, Canada, where he is currently a Professor and the Associate Director. In 2012, he visited University of Erlangen-Nuremberg, Germany, as an Alexander von Humboldt Research Fellow.

Dr. Liang's research interests include Image and Video Coding, Multimedia Communications, Sparse Signal Processing, Computer Vision, and Machine Learning. He is currently an Associate Editor for the IEEE Transactions on Image Processing, IEEE Transactions on Circuits and Systems for Video Technology (TCSVT), Signal Processing: Image Communication, and EURASIP Journal on Image and Video Processing. He was also an Associate Editor of IEEE Signal Processing Letters. He received the 2014 IEEE TCSVT Best Associate Editor Award, 2014 SFU Dean of Graduate Studies Award for Excellence in Leadership, and 2015 Canada NSERC Discovery Accelerator Supplements (DAS) Award.